Fractional-Order Control on PX4 Firmware: Open-Source Implementation for Fully-Actuated Hexa-Rotors

Andrés Montes de Oca
Department of Biological and Agricultural Engineering, UC Davis, Davis, CA 95616, USA

Alejandro Flores
Stemmer-Imaging, Queretaro, Qro 76090, Mexico

Micky Rakotondrabe, Member, IEEE
Systems Department, Laboratoire Génie de Production, University of Technology of Tarbes Occitanie Pyrénées (UTTOP), Tarbes, Hautes-Pyrénées 65000 France

Aldo Muñoz-Vázquez, Senior Member, IEEE
Department of Multidisciplinary Engineering, Texas A&M University, McAllen, TX 78504, USA

Gerardo Flores, Senior Member, IEEE
School of Engineering, College of Arts and Sciences, Texas A&M Int. University, Laredo, TX 78041 USA

This supplementary document includes further comparative results of the proposed FOC and other robust techniques and FOCs from the state-of-the-art. Additionally, a brief comparative is presented to highlight the implementation of desired position and velocity states in the proposed FOC.

A. Comparative Results

The previous subsection focused on a baseline comparison between the proposed fractional-order controller (FOC) and a classical PID controller using the ITSE

(Corresponding author: G. Flores, e-mail: gerardo.flores@tamu.edu).

A. Montes de Oca is with the Department of Biological and Agricultural Engineering, UC Davis, Davis, CA 95616, USA (e-mail: amoreb@ucdavis.edu). A. Flores is with Stemmer-Imaging, Queretaro, Qro 76090, Mexico (e-mail: a.flores@stemmer-imaging.com). M. Rakotondrabe is with the Systems Department, Laboratoire Génie de Production, University of Technology of Tarbes Occitanie Pyrénées (UTTOP), University of Toulouse alliance, Hautes-Pyrénées 65000 France (e-mail: mrakoton@uttop.fr). A. Muñoz-Vázquez is with the Department of Multidisciplinary Engineering, Texas A&M University, McAllen, TX 78504, USA (e-mail: aldo.munoz-vazquez@tamu.edu). G. Flores is with the School of Engineering, College of Arts and Sciences, Texas A&M Int. University, Laredo, TX 78041 USA (e-mail: gerardo.flores@tamu.edu)

metric. While those results validated the nominal performance advantage of the FOC, they did not account for more realistic operating conditions or alternative control strategies.

In this subsection, we extend the analysis by conducting a more comprehensive comparative study. To assess the performance and robustness of the proposed FOC, we designed a benchmark scenario in which all control strategies are evaluated under identical simulation conditions. The experiments are conducted on a fully-actuated multirotor operating in a 3D environment, with additive external disturbances applied to both position and orientation dynamics. The proposed FOC is compared against four representative control strategies from the literature: a fractional-order backstepping sliding mode controller (FOBSMC) [1], an adaptive fractional-order nonsingular fast terminal sliding mode controller (AFON-FTSMC) [2], a PID controller augmented with feedforward compensation (PID+FF), and a popular geometric control approach based on [3]. This configuration enables a fair and comprehensive evaluation of the proposed controller in terms of tracking performance, control effort, and robustness.

1. System Configuration

To evaluate the controllers under realistic conditions, additive Gaussian noise was introduced into the position disturbance signal, as illustrated in Fig. 1. The noise was generated using MATLAB's `Random Number` block, configured with zero mean, unit variance, and a sampling time of 0.01 s (see Fig. 1(a)). To ensure reproducibility and stochastic consistency across all simulations, independent noise signals were assigned to each position axis using fixed random seeds: 42 for the x-axis, 70 for the y-axis, and 98 for the z-axis.
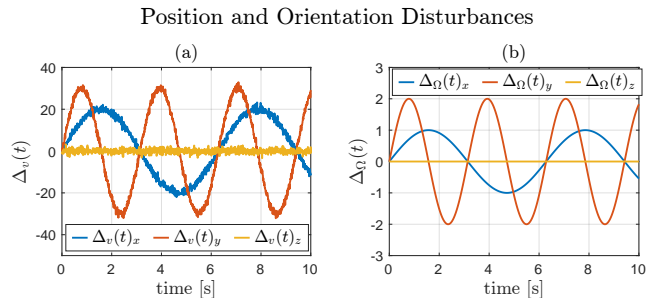
Position and Orientation Disturbances

Fig. 1: Additive external disturbances used in all experiments. Subfigure (a) shows the position disturbances $\Delta_v(t)$ along the x, y, and z axes, including injected Gaussian noise. Subfigure (b) displays the orientation disturbances $\Delta_\Omega(t)$. These signals were applied consistently across all control strategies to ensure fair robustness comparison.

The initial states were defined as follows:

- Position: $p(0) = [2, \ -1, \ 1.5]^\top$ (m)
- Linear velocity: $v(0) = [0, \ 0, \ 0]^\top$ (m/s)
- Orientation (Euler angles): $[10°, \ -15°, \ 5°]$

Comparison of tracking errors and control inputs from four benchmark control strategies
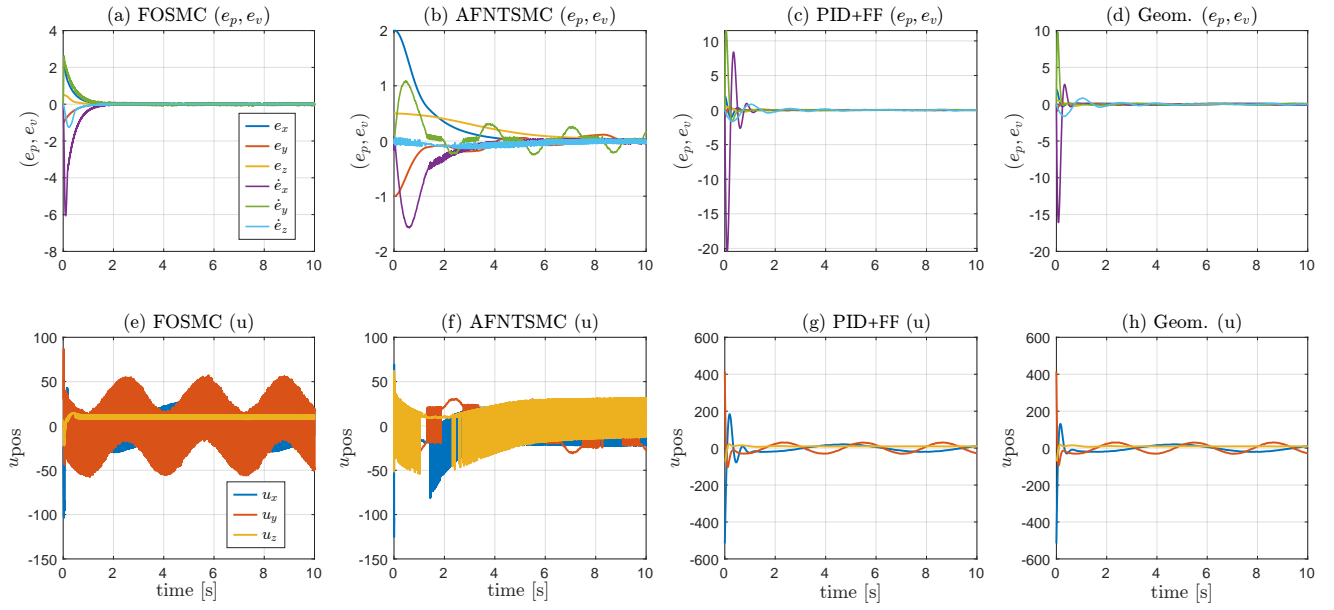

Fig. 2: Comparison of tracking performance and control effort for four benchmark control strategies under identical additive disturbances in position and orientation. Subfigures (a)–(d) show the evolution of position and velocity tracking errors (e_p, e_v) for FOSMC, AFNTSMC, PID+FF, and geometric controllers, respectively. Subfigures (e)–(h) present the corresponding control inputs u_x, u_y, and u_z for each strategy. Gaussian noise was included in the position disturbance to emphasize robustness assessment.

- Angular velocity: $\Omega(0) = [0,\ 0,\ 0]^\top$ (rad/s)

The UAV system parameters used in the comparison simulation were the same as in Table **??**. The simulation time was fixed at $T_s = 10$ seconds. The order of the fractional operator was set to $\alpha = 0.5$ for the proposed controller.

To ensure a fair comparison across all strategies, identical control gains were applied to the shared structure of each method: $K_1 = \text{diag}(220,\ 500,\ 20)$, $K_2 = \text{diag}(15,\ 34,\ 2)$, $\Lambda = \text{diag}(1.0,\ 0.05,\ 1.5)$. For state-of-the-art strategies requiring additional tuning parameters, these were adjusted only to avoid excessive control effort and overshoot, while preserving response quality.

2. Results Overview and Qualitative Performance Comparison

The results in Fig. 2 provide a qualitative comparison of tracking performance and control effort among four benchmark controllers under identical external disturbances. The fractional-order controllers (FOSMC and AFNTSMC), shown in subfigures (a)–(b) for tracking errors and (e)–(f) for control signals, exhibit excessive chattering in the inputs u_x, u_y, and u_z, particularly under strong additive noise. In Fig. 2(b), the AFNTSMC fails to fully reject the perturbations, resulting in persistent oscillations in the tracking errors and lack of convergence to zero. Although such errors could be reduced by increasing the controller gains, this leads to substantially higher control efforts, as seen in Fig. 2(f). Moreover, the AFNTSMC includes a large number of tuning parameters, making the

controller design and calibration process highly intricate and impractical for real-world implementation.

In contrast, the non-fractional controllers—PID with feedforward compensation (PID+FF) and the geometric controller—do not exhibit chattering, as illustrated in Figs. 2(g)–(h). However, these controllers produce excessive overshoots in the control signals during the transient phase and maintain residual oscillations in the tracking errors (Figs. 2(c)–(d)). These observations reveal a trade-off: while classical controllers yield smoother control signals, they struggle with robustness and precise convergence in noisy and highly perturbed environments.

Figure 3 illustrates the performance of the proposed fractional-order controller (FOC) under the same disturbance conditions applied to the benchmark controllers. Notably, the FOC achieves rapid and smooth convergence of both position and velocity tracking errors to zero, as depicted in Fig. 3 (a). The corresponding control inputs, shown in Fig. 3 (b), remain continuous and free from chattering. Although small oscillations are observed in the control signals, these are not due to discontinuous control actions but are rather the result of the injected Gaussian noise in the position disturbance channel. This behavior confirms the controller's robustness and its ability to maintain stable operation under high-magnitude perturbations.

3. Quantitative Performance Comparison

This subsection presents a quantitative evaluation of the tracking performance, control effort, and robustness
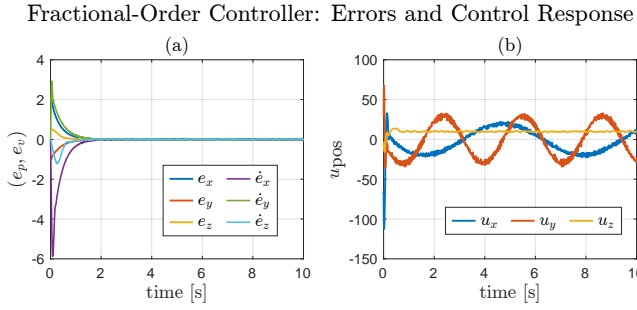
Fractional-Order Controller: Errors and Control Response

Fig. 3: Tracking errors (e_p, e_v) and control inputs $u_{\text{pos}} := -\frac{1}{m}R\mu = [u_x, u_y, u_z]^\top$ generated by the proposed fractional-order controller under additive disturbances in both position and orientation. Subfigure (a) shows the evolution of position and velocity errors; (b) depicts the corresponding control signals. Gaussian noise was added to the position signal to test robustness, explaining the observed fluctuations in the control inputs; these are not chattering artifacts but responses to the noisy position signals.

for all benchmark controllers, as summarized in Table I. The metrics used include the Mean Absolute Error (MAE), Mean Square Error (MSE), steady-state MSE (MSE_{ss}), Integral of Absolute Error (IAE), Integral of Time Square Error (ITSE), and Integral of Time Absolute Error (ITAE), which together characterize the tracking accuracy and convergence speed. Additionally, the root mean square of the control effort (U_{rms}), the Total Variation of Control (TVC), and the Disturbance-to-Error Energy Ratio (DEER) are used to quantify control smoothness and disturbance rejection.

From the table, it is evident that the proposed FOC achieves the lowest IAE, ITSE, and ITAE among all controllers, indicating faster and more precise convergence. It also presents the smallest MSE_{ss}, demonstrating superior steady-state accuracy. While the AFONFTSMC obtains the best overall MSE, its performance suffers from high overshoot and parameter complexity, as noted earlier. In contrast, the PID+FF and geometric controllers avoid chattering but show poor performance in IAE, ITSE, and DEER due to overshoot and residual oscillations. Moreover, the proposed FOC offers the lowest TVC and control effort, confirming its efficiency and robustness under additive disturbances.

In summary, the proposed fractional-order controller (FOC) demonstrates superior performance across all evaluated criteria when compared to both fractional and nonlinear benchmark controllers. It consistently achieves lower tracking errors, smoother control signals, and better

disturbance rejection, particularly under challenging conditions involving additive Gaussian noise. Unlike other fractional-order approaches, which suffer from excessive chattering or parameter tuning complexity, the proposed method balances performance and practicality. Moreover, it outperforms conventional PID-based methods by ensuring faster convergence, reduced control effort, and improved robustness.

I. Effect of using $\dot{p}_d, \ddot{p}_d$ in the proposed FOC.

Finally, the impact of using $\dot{p}_d$ and $\ddot{p}_d$ in the control law is evaluated. For this, a comparison is made between two SITL simulations. The results can be seen in Fig. 4. This figure depicts the position states (x, y) response in two cases: a) using only x_d and b) using x_d, $\dot{p}_d$, and $\ddot{p}_d$. The second case shows that the position states are less noisy and close to the reference in a path tracking scenario.
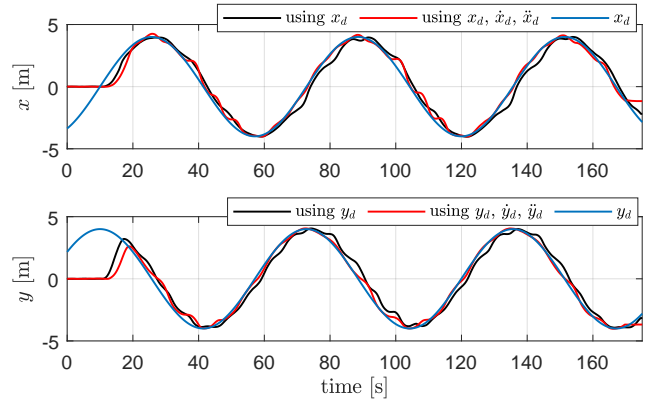

Fig. 4: Path tracking results showing the importance of using $\dot{p}_d$ and $\ddot{p}_d$ terms in the control law.

REFERENCES

[1] C. Yin, B. Hu, Y. Cheng, J. Xue, and X. Shi, "Design of fractional-order backstepping sliding mode controller for the quadrotor unmanned aerial vehicles," in *2018 37th Chinese Control Conference (CCC)*, 2018, pp. 697–702.

[2] M. Labbadi and M. Cherkaoui, "Adaptive fractional-order non-singular fast terminal sliding mode based robust tracking control of quadrotor UAV with Gaussian random disturbances and uncertainties," *IEEE Transactions on Aerospace and Electronic Systems*, vol. 57, no. 4, pp. 2265–2277, 2021.

[3] T. Lee, M. Leok, and N. H. McClamroch, "Geometric tracking control of a quadrotor UAV on SE(3)," in *49th IEEE Conference on Decision and Control (CDC)*, 2010, pp. 5420–5425.

TABLE I: Quantitative comparison of tracking performance, control effort, and robustness against external disturbances based on $e = [e_p; e_v]$.

Metric	Proposed FOC	FOBSMC [1]	AFONFTSMC [2]	PID+FF	Geometric [3]
MAE	**0.5143**	0.5579	1.044	0.8543	0.8489
MSE	0.854	0.8902	**0.6995**	3.857	3.85
MSE_{ss}	$\mathbf{6.605 \times 10^{-4}}$	2.511×10^{-2}	9.422×10^{-2}	2.55×10^{-2}	2.483×10^{-2}
IAE	**0.2669**	0.3109	0.5279	0.5226	0.5189
ITSE	**0.1742**	0.3002	0.6821	0.529	0.5241
ITAE	**0.3684**	0.6037	2.371	1.636	1.624
U_{rms}	**28.59**	45.45	40.41	41.95	41.95
TVC	**55.85**	4.147e+04	3.769e+04	157.7	157.7
DEER	1.341×10^{-3}	1.398×10^{-3}	$\mathbf{1.098 \times 10^{-3}}$	6.056×10^{-3}	6.046×10^{-3}